JVI Journals.ASM.org

APOBEC3 Deaminases Induce Hypermutation in Human Papillomavirus 16 DNA upon Beta Interferon Stimulation

Zhe Wang,[a] Kousho Wakae,[a] Kouichi Kitamura,[a] Satoru Aoyama,[a] Guangyan Liu,[a] Miki Koura,[a] Ahasan M. Monjurul,[a] Iwao Kukimoto,[b] Masamichi Muramatsu[a]

Department of Molecular Genetics, Kanazawa University Graduate School of Medical Sciences, Kanazawa, Japan[a]; Pathogen Genomics Center, National Institute of Infectious Diseases, Musashimurayama, Tokyo, Japan[b]

Apolipoprotein B mRNA-editing catalytic polypeptide 3 (APOBEC3) proteins are interferon (IFN)-inducible antiviral factors that counteract various viruses such as hepatitis B virus (HBV) and human immunodeficiency virus type 1 (HIV-1) by inducing cytidine (C)-to-uracil (U) mutations in viral DNA and inhibiting reverse transcription. However, whether APOBEC3 proteins (A3s) can hypermutate human papillomavirus (HPV) viral DNA and exhibit antiviral activity in human keratinocyte remains unknown. Here we examined the involvement of A3s in the HPV life cycle using cervical keratinocyte W12 cells, which are derived from low-grade lesions and retain episomal HPV16 genomes in their nuclei. We focused on the viral E2 gene as a potential target for A3-mediated hypermutation because this gene is frequently found as a boundary sequence in integrated viral DNA. Treatment of W12 cells with beta interferon (IFN-β) increased expression levels of A3s such as A3A, A3F, and A3G and induced C-to-U conversions in the E2 gene in a manner depending on inhibition of uracil DNA glycosylase. Exogenous expression of A3A and A3G also induced E2 hypermutation in W12 cells. IFN-β-induced hypermutation was blocked by transfection of small interfering RNAs against A3G (and modestly by those against A3A). However, the HPV16 episome level was not affected by overexpression of A3A and A3G in W12 cells. This study demonstrates that endogenous A3s upregulated by IFN-β induce E2 hypermutation of HPV16 in cervical keratinocytes, and a pathogenic consequence of E2 hypermutation is discussed.

Apolipoprotein B mRNA-editing catalytic polypeptide (APOBEC) proteins are a family of proteins that share cytidine deaminase activity of DNA and RNA. In humans, the APOBEC family is composed of at least 11 members, including activation-induced cytidine deaminase (AID) and APOBEC1, -2, -3A, -3B, -3C, -3DE, -3F, -3G, -3H, and -4 (1, 2). AID introduces cytidine (C)-to-uracil (U) conversion in immunoglobulin (Ig) genes, a step that is further catalyzed by downstream DNA repair machineries, including base excision repair (BER), mismatch repair, and nonhomologous end-joining repair, to trigger somatic hypermutation, class switch recombination, gene conversion, and chromosomal translocation (3–6). AID also introduces mutations in non-Ig gene loci, such as *c-Myc* and *Bcl-6*, although less frequently than in Ig genes (3, 7). Recent studies have suggested that APOBEC3 protein (A3) deaminase activity is responsible for a novel type of mutations called kataegis in multiple human cancers, including cancers of the bladder, cervix, lung, head and neck, and breast (8–13).

A3s are antiviral factors against viruses and transposable elements that use reverse transcription during their life cycle (1, 2, 14–16). The antiviral functions of A3s have been extensively studied for human immunodeficiency virus type 1 (HIV-1) and hepatitis B virus (HBV). APOBEC3G (A3G) physically associates with viral RNP complexes, including viral genomic RNA, gag protein (in the case of HIV-1), and P and core protein (in the case of HBV), and is encapsidated into a nucleocapsid, thereby inhibiting reverse transcription in infected cells (2, 14, 17). Moreover, A3G-induced hypermutation in viral DNA leads to inhibition of HIV-1 replication by either BER-mediated DNA degradation or accumulation of destructive mutations in the viral genome (16, 18–20). How C-to-U conversion in cellular or viral DNA is converted into different genetic alterations (hypermutation, recombination, and DNA degradation) remains unknown.

Human papillomaviruses (HPVs) are small double-stranded DNA viruses infecting epithelial cells. A subset of mucosal HPVs is recognized as a causative agent of cervical cancer (21, 22), among which HPV16 accounts for at least 50% of cervical cancer cases worldwide (23). The HPV16 genome is a 7.9-kb closed circular DNA and is composed of at least 8 open reading frames (E1, E2, E4, E5, E6, E7, L1, and L2) as well as the noncoding long control region (LCR). LCR contains the replication origin and the P_{97} promoter responsible for transcription of the E6 and E7 genes. E6 and E7 are viral oncoproteins that degrade p53 and retinoblastoma proteins, respectively, and their enhanced expression is required for cellular transformation (22). In its normal life cycle, HPV16 infects the basal cells of cervical epithelia and establishes their genomes as extrachromosomal episomes. In invasive cervical cancer, however, the viral DNA is frequently integrated into the host chromosome, which generally leads to constitutive expression of E6 and E7. The viral DNA integration often results in disruption of the E2 gene and loss of E2 expression. This disruption of the E2 gene causes upregulation of E6/E7 expression because E2 is a transcriptional repressor of the P_{97} promoter responsible for E6/E7 expression. Although viral DNA integration is an important step in HPV-induced carcinogenesis (24, 25), a mechanism of HPV integration remains unknown.

A3s can also target DNA viruses that do not use reverse transcription in their replication cycle, including TT virus, adeno-

Received 4 November 2013 Accepted 5 November 2013
Published ahead of print 15 November 2013
Address correspondence to Masamichi Muramatsu, muramatsu@med.kanazawa-u.ac.jp.

doi:10.1128/JVI.03091-13

associated virus (AAV), herpes simplex virus 1 (HSV-1), and Epstein-Barr virus (26–30). To date, only a single study of A3-mediated hypermutation in HPV has been reported (31), in which Vartanian et al. detected hypermutation in the LCR of the HPV16 DNA isolated from clinical specimens of cervical precancerous lesions. They further demonstrated the LCR hypermutation in HPV1a DNA isolated from 293T cells transfected with an HPV plasmid and A3 expression vectors. However, Stenglein et al. recently demonstrated that transfected plasmids were hypermutated in the presence of overexpressed A3s except A3G (32), raising a concern about whether the observed hypermutation in the transfected HPV DNA truly reflects HPV pathophysiology.

In this study, we utilized cervical keratinocyte W12 cells that are derived from low-grade cervical intraepithelial lesions caused by natural infection of HPV16 and represent a unique model system for studying early events in HPV persistent infection (33, 34). Using the W12 system, we investigated whether A3s induce hypermutation in HPV16 DNA and exhibit antiviral activity against HPV16.

MATERIALS AND METHODS

Reagents and cell culturing. Beta interferon (IFN-β) and tamoxifen were purchased from Daiichi Sankyo and Wako, respectively. W12 (20863 clone) cells were maintained as reported previously (33, 35). In brief, W12 cells were cocultured with mitomycin C-treated 3T3 feeder cells in F medium composed of 3 parts F-12 medium and 1 part Dulbecco's modified Eagle's medium supplemented with 5% fetal bovine serum, 5 μg/ml of insulin, 8.4 ng/ml of cholera toxin, 24 μg/ml of adenine, 10 ng/ml of epidermal growth factor, 0.4 μg/ml of hydrocortisone, and 100 U/ml penicillin, and 100 mg/ml streptomycin. W12 cells were infected with UNG inhibitor-estrogen receptor (UGI-ER)-expressing retroviruses, and transduced cells were further selected by puromycin (36, 37) using puromycin-resistant feeder cells. Plasmids were transfected into W12 cells using Fugene 6 (Roche), according to the manufacturer's instructions. All small interfering RNAs (siRNAs) were purchased from Invitrogen and were transfected into W12 cells using Lipofectamine 2000 (Invitrogen), according to the manufacturer's instructions.

Plasmids. A mock-estrogen receptor (mock-ER) expression vector was made by replacing the AID gene in pCMV-AID-ER (38) with linker DNA containing an in-frame ATG. This vector expresses a 36-kDa mock-ER protein. Human A3A- and A3G-ER expression vectors were made by replacing the AID gene in pCMV-AID-ER with the A3A and A3G genes in frame. DNA fragments encoding human A3A and A3F were generated by reverse transcription-PCR (RT-PCR) using primers A3A fwd, 5′-ATAGAATTCATGGAAGCCAGCCCAGC-3′, A3A rev, 5′-ATATCTCGAGTCAGTTCCCTGATTCT-3′, A3F fwd, 5′-ATTTAAGCTTATGAAGCCTCACTTCAG-3′, and A3F rev, 5′-AATTCTCGAGTCATTCGAGAATCTCCTGCAG-3′, and inserted into a multiple cloning site of pcDNA3Tag1A (Invitrogen) to make FLAG-tagged A3A and A3F expression vectors, respectively. The A3G nontagged protein expression vector was made by deletion of FLAG region from pFlag-A3G (37). Differential DNA denaturation PCR (3D-PCR) control vectors were generated by cloning PCR fragments into the pGEM-T Easy vector (Promega). Briefly, the E2 PCR fragments were amplified with #888 and #843 E2 primers (Table 1) from total DNA isolated from W12 cells using a 3D-PCR protocol. Plasmids which contain no mutations (negative control [n.c.]), 4 C-to-T mutations (4× positive control [p.c.]), or 26 C-to-T mutations (26× p.c.) were used as controls. Control DNAs for LCR and *TP53* 3D-PCR were also generated using primers described elsewhere (31, 39). All the plasmids used in this study were sequenced at least once to verify them. Other plasmids used in this study have been described previously (37, 40).

Detection of hypermutation in E2, LCR, and *TP53*. Total DNA was extracted by a standard method. In brief, cells were digested with buffer containing 200 μg/ml proteinase K, 1% (vol/vol) sodium dodecyl sulfate, 150 mM NaCl, 25 mM EDTA, and 50 mM Tris-HCl (pH 8.0) at 55°C overnight. Total DNA was purified by phenol-chloroform extraction, treated with RNase A to remove RNA, and further purified by phenol-chloroform extraction and ethanol precipitation. E2 3D-PCR was performed by modification of a previously published method (41, 42). The initial PCR was performed as follows: 94°C for 4 min, followed by 35 cycles, each at 94°C for 16 s, 55°C for 20 s, and 68°C for 50 s, and a final elongation step at 65°C for 10 min, using #908 and #845 primers (Table 1). Nested PCR was performed as follows: 86.9 to 82.6°C for 5 min, followed by 35 cycles, each at 86.9 to 82.6°C for 45 s, 50°C for 30 s, and 65°C for 38 s, and a final elongation step at 65°C for 10 min, using #888 and #843 primers, on a MasterCycler Pro thermal cycler (Eppendorf). The nested PCR amplified an E2 gene fragment (nucleotide number 3400-3564) in HPV genomic DNA (GenBank accession number AF125673). LCR and *TP53* 3D-PCR were performed as described previously (31, 39), with minor modifications. rTaq (TaKaRa) was used for PCRs for both 3D-PCR and estimation of mutation load, because high-fidelity DNA polymerase cannot amplify uracilated DNA. To determine the hypermutation frequency, PCR fragments from 3D-PCR or standard PCR (94°C denaturation) were cloned into a T vector, and the indicated number of successful recombinant clones were selected randomly and sequenced using an ABI Prism 3130 (Applied Biosystems). The W12 HPV16 sequence (GenBank accession number AF125673) was used as a reference sequence to examine the presence of mutations.

TABLE 1 3D-PCR assay primer list

Primer[a]	Sequence (5′−3′)
First F (#908)	ATGGGAAGTTCATGCGGGTGGTCA
First R (#845)	TGGGTGTAGTGTTACTATTACAGTTAAT
Second F (#843)	TCCTGAAATTATTAGGCAGCACTT
Second R (#888)	CGTCCTTTGTGTGAGCTGTTAAAT

[a] F, forward; R, reverse.

RT-qPCR. cDNAs were prepared as reported previously (37, 40). In brief, total RNA was extracted and treated with DNase I to digest genomic DNA. For reverse transcription-quantitative PCR (RT-qPCR) analysis, total RNA was again treated with amplification-grade DNase I (Invitrogen) and reverse transcribed using SuperScript III (Invitrogen). The cDNA was amplified using specific primers for A3A, A3B, A3C, A3DE, A3F, A3G, A3H, AID, APOBEC1 (A1), and hypoxanthine phosphoribosyltransferase (HPRT) (37, 40). To calculate relative A3 expression levels, serially diluted plasmids containing each A3 gene were used to form a standard curve. Expression of HPRT was used to normalize expression levels of A3s under different culture conditions. RT-PCR analysis to determine ISG54 expression were performed with primers 5′-GAGAACTGCAATGTTTCAGGACC-3′ and 5′-TGTATAGTTGTTTGCAGCTGTGTGC-3′. ISG56 primers have been shown previously (43).

Southern blotting and Western blotting. DNA probes spanning the entire HPV16 viral genome (GenBank accession number NC_001526) were generated by PCR using primer pairs #765/836 and #928/1111 (Table 2). A DNA probe that recognizes a human genomic locus (AICDA) was generated by PCR primer pairs #1124/1165 (Table 2) and used to determine the amount of DNA loaded per gel in Southern blotting. Probe labeling and signal development were performed using the AlkPhos direct labeling system (Amersham), and the signals were detected using the LAS1000 imager system (FujiFilm). Western blotting was performed using a standard method as described previously (37, 40). The antibodies used in this study were as follows: rabbit anti-A3G (37), rabbit anti-GAPDH (glyceraldehyde-3-phosphate dehydrogenase) (G9545; Sigma), rabbit anti-ER (HC-20; Santa Cruz), anti-rabbit IgG-horseradish peroxidase (HRP) (ALI3404; eBioscience), mouse anti-FLAG (M2; Sigma), anti-mouse IgG-HRP (GE Healthcare), and anti-HA (ab-HAtag; InvivoGen).

UNG assay. A uracil DNA glycosylase (UNG) assay was performed as described previously (37, 44).

TABLE 2 Primer list for making Southern blot probes

Primer[a]	Sequence (5′−3′)
HPV16	
F, #765	TGCTTGCCAACCATTCCATTGTTTTTT
R, #836	AGCGGACGTATTAATAGGCAGA
F, #928	ACAGCAGCCTCTGCGTTTAG
R, #1111	CGTCCTAAAGGAAACTGATC
Loading control	
F, #1124	AGTGGCCTAAACACCACATTAAAGA
R, #1165	GCGTGTGCCACGGTTCGCAGCTTT

[a] F, forward; R, reverse.

Statistical analysis. Statistical analyses were performed using GraphPad Prism (GraphPad software). Analysis of variance (ANOVA) was used for RT-qPCR data. Pearson's chi-square test was used for mutation analyses. *P* values of less than 0.05 between experimental groups were considered statistically significant. For all graphs in this study, error bars indicate the standard errors of the means from triplicate samples.

RESULTS

Induction of APOBEC3 genes by IFN-β stimulation. One of the type I IFNs, IFN-β, has been shown to repress HPV DNA replication in keratinocyte cell lines, including W12 cells (35, 45, 46). Because A3s are IFN-inducible antiviral factors against retroviruses and HBV (1, 2, 14, 16, 37), we aimed to explore the involvement of A3s in the IFN-β action against HPV. We first examined basal expression levels of each A3 gene in W12 cells. RT-qPCR analysis showed that all seven A3s were expressed at different levels: A3C and A3G were the highest; A3A, A3DE, and A3H were intermediate; and the lowest were A3B and A3F (Fig. 1A). We then examined which A3 member is induced upon IFN-β treatment in W12 cells. RT-qPCR revealed that IFN-β treatment upregulated mRNA levels of most A3s, including A3A, A3F, and A3G, in W12 cells (Fig. 1B). Increased expression of A3G protein by IFN-β was also confirmed by Western blotting (Fig. 1C). However, available antibodies did not detect endogenous A3A protein in IFN-β stimulated W12 cells (data not shown). Putative type I IFN-responsive genes IFN-stimulated gene 54 (ISG54) and ISG56 (also known as *IFIT2* and *IFIT1*, respectively) (47) were also upregulated (Fig. 1D), suggesting that a signaling pathway of IFN-β is operative in W12 cells. Other APOBEC family members APOBEC1 and AID were not expressed in the IFN-β-stimulated and nonstimulated W12 cells (Fig. 1A).

APOBEC3A and -3G hypermutate the HPV16 E2 gene. In the case of HBV infection, expression of A3s in the infected hepatocytes, either by overexpression of these proteins or through IFN stimulation, leads to hypermutation of viral DNA (2, 16, 37, 40, 42, 48, 49). We investigated whether A3s can hypermutate HPV16 DNA. To this end, we evaluated the effects of A3A, A3F, and A3G because expression of these A3s is induced by IFN-β stimulation in W12 cells (Fig. 1B). First, we simply overexpressed A3A, A3F, and A3G in W12 cells. HPV16 LCR DNA from these cells was cloned into a T vector, and 10 clones were sequenced; however, we did not see any sign of hypermutation (data not shown).

Then we applied 3D-PCR assay that can detect hypermutated DNA with higher detection sensitivity by decreasing the denaturation temperature in a PCR. Since Vartanian et al. (31) reported hypermutation in the LCR of HPV genomes by 3D-PCR assay, we chose the same region, using total DNA isolated from A3A- and A3G-expressing W12 cells. However, we did not see any evidence of hypermutation in the HPV16 LCR in these transfectants (data not shown). To establish another 3D-PCR assay, we chose the E2 gene. Importantly, mutation in the E2 gene may impair E2 gene functions, which is considered to be associated with progression of HPV-associated carcinogenesis. Moreover, the E2 gene is frequently found as a boundary sequence in integrated viral DNA (21, 24, 25, 50). In the first trial of the E2 3D-PCR assay, the A3-estrogen receptor (ER) fusion proteins were expressed in W12 cells as an inactive form, and then A3-ER proteins were activated by addition of an ER ligand, 4-hydroxytamoxifen (OHT) (51). The E2 genes from the A3A and A3G transfectants were amplified at a slightly lower denaturation temperature (85.6°C) than those from mock transfectants (86.0°C) and a negative-control DNA (n.c.) carrying no mutations (86.4°C) (Fig. 2A). Western blot results confirmed transgene expression levels (Fig. 2B). DNAs amplified at 85.6°C as shown in Fig. 2A were cloned into a T vector, and DNA sequence was determined. Results indicated that A3A and A3G induce low levels of hypermutation in the E2 gene (Fig. 2C and D).

Since the predominance of uracil DNA glycosylase (UNG) activity over cytidine deaminase activity may mask a hypermutation event, we utilized an inducible inhibition system of cellular UNG. We controlled UNG activity by expression of the UNG inhibitor protein (UGI). UGI is an irreversible inhibitor that forms an ex-

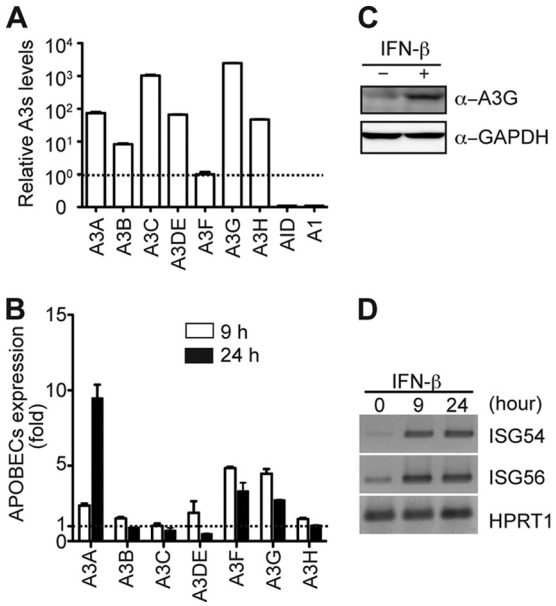

FIG 1 IFN-β induces APOBEC3 expression in W12 cells. (A) Expression levels of A3s in untreated W12 cells. Quantitative PCR (qPCR) was performed with primers to detect A3s using cDNA synthesized from transcripts derived from untreated W12 cells and control plasmids containing DNA from each A3 protein. Using standard curves for each A3 protein, copy number was determined. The relative expression level of A3F was defined as 1. qPCR did not detect significant expression of AID and APOBEC1 in W12 cells. (B) Expression of A3 genes at 9 and 24 h of IFN-β (1,000 U/ml) stimulation was compared with that of untreated W12 cells. Expression of untreated W12 cells was defined as 1, and expression of treated cells was described as a fold change relative to untreated cells. (C) A3G protein expression in IFN-β (1,000 U/ml)-treated W12 cells for 3 days was determined by Western blotting. Anti-GAPDH was used as a loading control. α, anti. (D) RT-PCR of ISG54 and -56 was performed using RNA identical to that used for panel B.

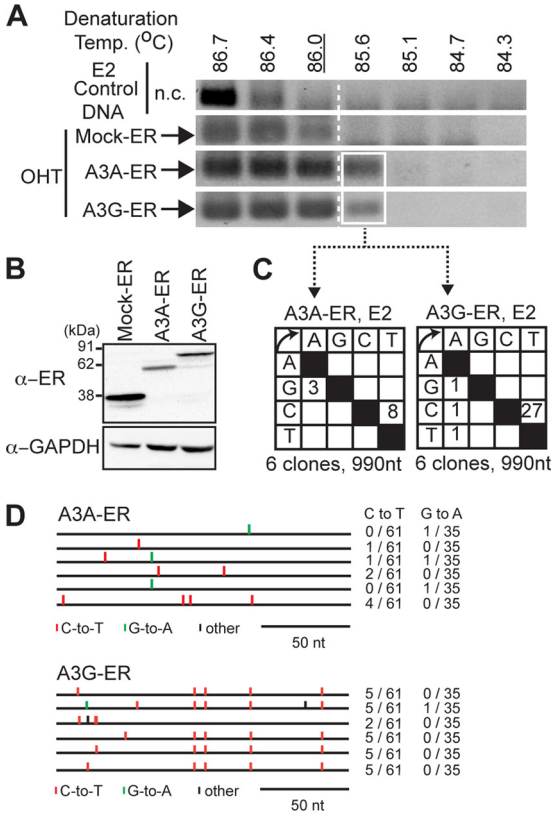

FIG 2 Expression of A3A and A3G induces hypermutation of the E2 gene in W12 cells. (A) A3A-, A3G-, and mock-ER proteins were expressed in W12 cells. Transfectants were cultured in the presence of 1 μM OHT for 36 h, and total DNA was subjected to E2 3D-PCR assays. A3A- and A3G-ER transfectants showed amplification at a denaturation temperature (85.6°C), slightly lower than those of the mock-ER transfectants (86.0°C) and control DNA (86.4°C). Arrows indicate the position of 3D-PCR products (213 bp). Negative-control (n.c.) DNA carrying no mutations was also examined. (B) Expression of mock-, A3A-, and A3G-ER proteins was verified by Western blotting. GAPDH served as a loading control. (C and D) E2 DNA amplified at a denaturation temperature of 85.6°C was excised, cloned, and sequenced. Results are shown as mutation matrices (C) and alignments (D). C-to-T and G-to-A hypermutations are indicated as red and green vertical lines, respectively. All other base substitutions are shown as black vertical lines. The number of C-to-T and G-to-A conversions in each sequence is indicated. nt, nucleotides.

ceptionally stable complex with the UNG protein (37, 44). We generated a W12 cell line that stably expresses the UGI-ER fusion protein (Fig. 3A). We had previously demonstrated that addition of OHT to the culture medium activated inhibitory activity of the UGI-ER protein (37, 44). As shown in Fig. 3B, our UNG assay revealed that OHT stimulation of UGI-ER resulted in inhibition of UNG activity in W12 cells, although we observed residual UNG activity (16% to 0.5% of nontransfectants) in the lysate from UGI-activated W12 cells. Addition of OHT to parental W12 cells did not change UNG activity, indicating that OHT did not directly affect UNG activity (Fig. 3B, left).

The UGI-ER transfectants were then transiently transfected with FLAG-tagged A3A, A3F, or A3G expression vectors (or green fluorescent protein [GFP] as a negative control), and these transfectants were divided into OHT-stimulated and nonstimulated (EtOH) groups. Three days after transfection, total DNA was isolated, and E2 hypermutation was examined using the E2 3D-PCR assay. A control DNA (n.c.) carrying no mutations showed amplification with a denaturation temperature of up to 86.5°C (Fig. 3C). Another control DNA, carrying 4 C-to-T mutations (4× p.c.), showed amplification at up to 86.0°C. Any samples derived from W12 cells, regardless of the transgene expressed, amplified the E2 gene at 86.0°C (Fig. 3C), indicating the presence of the E2 gene with around 4 C-to-T mutations in all the transfected samples. Endogenous APOBEC3 proteins may be responsible for this background level (86.0°C) of hypermutation and may also be responsible for spontaneous cytosine deamination that occurs in mammalian genomic DNA (52). When A3A and A3G were expressed, we observed E2 amplification at a markedly lower denaturing temperature in the presence of UNG inhibition (Fig. 3C, OHT). A3A-expressing, UNG-inhibited W12 cells produced E2 gene amplification at up to 82.6°C, which is an equivalent temperature for amplification of a positive-control DNA carrying 26 C-to-T hypermutations. Of note, a mutant A3G (mutA3G) of deaminase active sites (E67Q/E259Q) (53) showed the same profile of amplification temperature with the GFP and EtOH controls, suggesting dependence on deaminase activity for hypermutation, as observed in A3G-expressing, UNG-inhibited W12 cells. To confirm E2 hypermutation, amplified E2 fragments (Fig. 3C, boxes) were excised and cloned into a T vector. Eight *Escherichia coli* clones were randomly picked up, followed by plasmid isolation and sequence determination of the amplified E2 fragments. Sequence analysis revealed robust C-to-T and G-to-A hypermutations in the A3A- and A3G-expressing samples (Fig. 3D). The positive strand of E2 3D-PCR target DNA (165 bp) contains 21 CpC and 8 TpC dinucleotides, whereas the negative strand contains 5 CpC and 13 TpC dinucleotides. It has been reported that A3A and A3G prefer T/CpC and CpC dinucleotide contexts, respectively (16, 32), and this is favored by our dinucleotide context analysis (Fig. 3E). Although the precise mechanism by which A3G causes a C-to-T-biased hypermutation is currently unknown, the biased distribution of the CpC dinucleotide context may partly account for it (Fig. 3D). OHT stimulation did not change the expression levels of A3A, A3G, and GFP (Fig. 3F). These results clearly demonstrate that overexpression of A3A and A3G induces hypermutation in the E2 gene, whereas UNG decreases the E2 hypermutation.

In addition, we tried to determine the overall mutation frequency of the E2 hypermutation. The first PCR product for E2 3D-PCR amplified from the same DNA sample that exhibited robust hypermutation by A3A (Fig. 3C) was cloned into the T vector, and the DNA sequence was subsequently determined. However, we saw no significant mutations among 50 clones (262 bp × 50) over background mutation due to *Taq* polymerase error (data not shown). This means that the majority of viral clones did not accumulate hypermutation in the E2 gene although the highly sensitive assay (3D-PCR) detected robust hypermutation in the same samples (Fig. 3C and D).

Detection of E2 hypermutation in the UNG-inhibited W12 cells encouraged us to further examine LCR hypermutation, using the same protocol of LCR 3D-PCR previously reported by Vartanian et al. (31). We examined the hypermutation load on the LCR in the identical samples used to detect E2 hypermutation (Fig. 3C). The LCR 3D-PCR clearly amplified a positive-control DNA, carrying 17 C-to-T mutations (17× p.c.), at a denaturation temperature of up to 79.4°C (Fig. 4A), whereas samples isolated from any transfectants except the A3A sample showed amplification

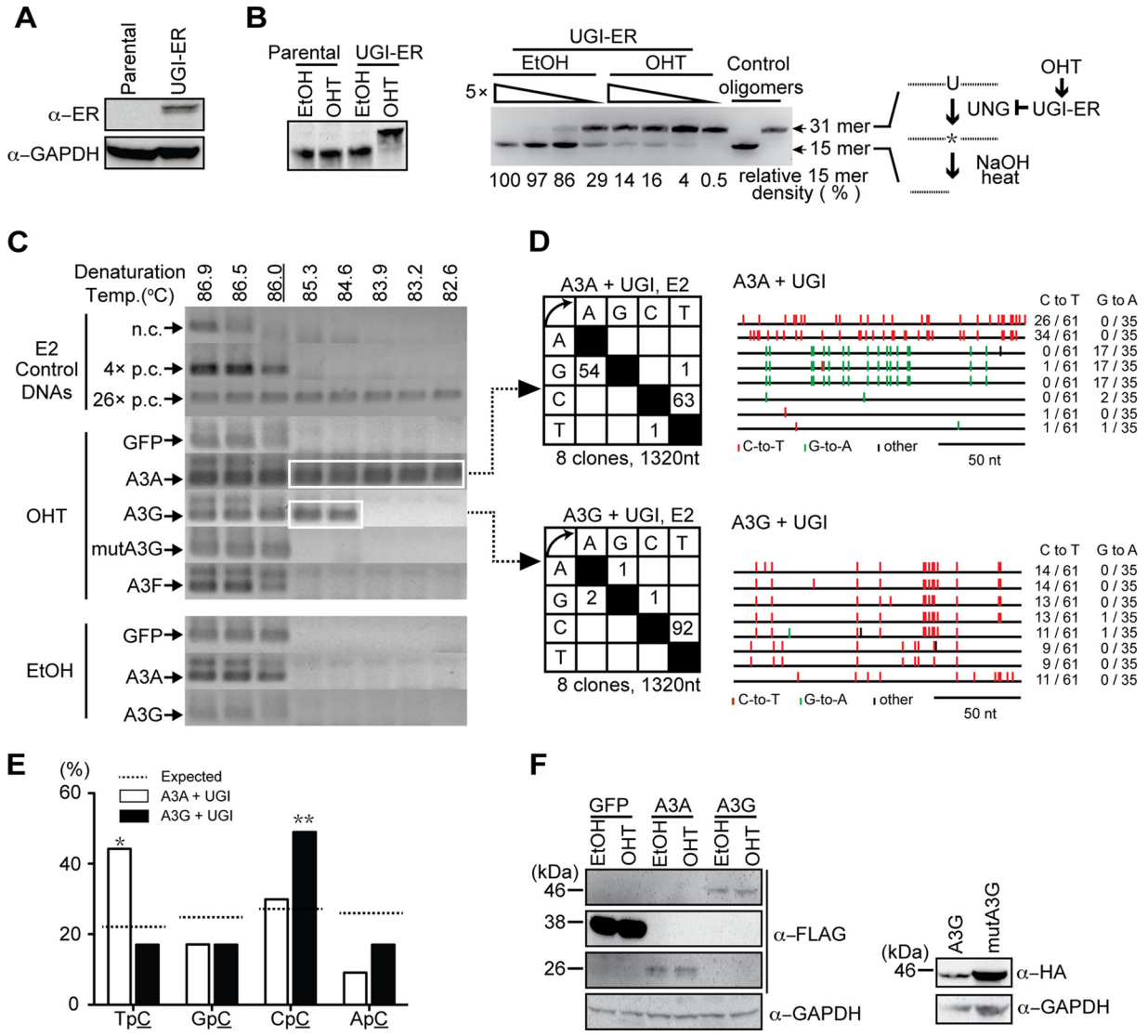

FIG 3 A3A and A3G heavily hypermutate the E2 gene in the UNG-inhibited W12 cells. (A) Protein expression in stable UGI-ER transfectants was confirmed by Western blotting. (B) Uracil excision activity was measured using a UNG assay with a synthetic single-stranded DNA containing a single dU. Parental and UGI-ER-expressing W12 cells were treated with either 1 μM OHT or the same amount of solvent (EtOH) for 48 h, and UNG activity was measured. Synthetic oligonucleotides (substrate, 31-mer, and control, 15-mer) were also electrophoresed as size markers. On the right side, UNG activity of serial dilutions of nuclear extracts was determined. The percent density of signals for the 15-mer is indicated. Signal density of the EtOH-treated UGI-ER-expressing W12 cells was defined as 100%. OHT stimulation decreased UNG activity in the UGI-ER transfectants. The asterisk represents an abasic site. On the left, uracil excision activity of parental W12 cells was compared. (C) Expression vectors of the indicated proteins were used to transfect UGI-ER transfectants. Twenty-four hours after transfection, 1 μM OHT (or EtOH) was added to activate the UGI-ER protein. After a further 72 h of incubation, total DNA was purified, and E2 3D-PCR assays were performed. Plasmids containing the E2 gene fragments carrying no (n.c.), 4 (4× p.c.), or 26 (26× p.c.) C-to-T mutations were simultaneously amplified and served as controls. Expression of A3A and A3G induced robust hypermutation in UNG-inhibited W12 cells. Arrows indicate the positions of E2 3D-PCR products (213 bp). (D and E) Summary of 3D-PCR amplicon sequences recovered from the work shown in panel C. Boxed PCR fragments described in panel C were excised and cloned into a T vector, and 8 randomly selected clones were sequenced. Results were shown as mutation matrices (D, left), alignments (D, right), and 5′-dinucleotide context analysis (E). *, $P < 0.05$; **, $P < 0.01$. The reference sequence (GenBank accession number AF125673.1) was used to identify mutations. (F) The levels of expressed proteins described in panel C were determined by Western blotting using the indicated antibodies. HA, hemagglutinin.

similar to that of the negative-control DNA, which carried no mutations. LCR DNA of the A3A sample amplified at 80.8°C (Fig. 4A, box) was excised and cloned in T vector, and subsequent DNA sequencing confirmed hypermutation (Fig. 4B and C). Dinucleotide context analysis of C-to-T mutations shows a TpC preference that is consistent with previous reports of A3A dinucleotide preference (Fig. 4D) (32, 54).

Suspene et al. and Mussil et al. (39, 54) demonstrated that A3A hypermutates host nuclear gene loci such as *TP53* and *c-myc* in activated T cells and UGI-expressing 293T cells. Because robust E2 hypermutation was detected in the A3A- and UGI-expressing W12 cells (Fig. 3C), we examined hypermutation in the *TP53* locus using the same DNA samples as those described in Fig. 3, 4A, and 5A. As shown in Fig. 4E, *TP53* 3D-PCR differentially amplified wild-type control DNA and one containing four C-to-T mutations. However, neither A3-dependent nor IFN-β-dependent

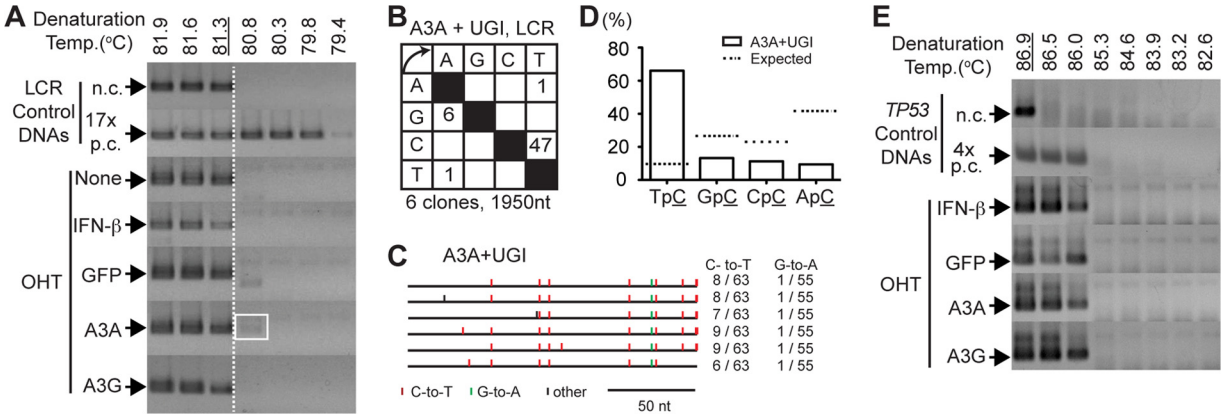

FIG 4 A3A expression causes LCR hypermutation in UGI-ER transfectants. (A) The total DNA samples used in Fig. 3C and 5A were analyzed in the LCR 3D-PCR assay. Control LCR 3D-PCRs were simultaneously carried out with the indicated control DNAs (n.c. and 17× p.c.); 17× p.c. and n.c. carry 17 C-to-T and no mutations in LCR DNA, respectively. The A3A-expressing sample showed a faint signal amplified at a denaturation temperature of 80.8°C (indicated by the open box). (B to D) The PCR signal indicated by the open box was cloned and sequenced. Results are shown as mutation matrices in panel B, alignments in panel C, and 5′-dinucleotide context analysis in panel D. (E) The same samples shown in panel A were also examined by *TP53* 3D-PCR assay. Control DNAs carrying no mutations (n.c.) and four C-to-T mutations (4× p.c.) were used simultaneously.

hypermutation was detected. Regardless of transgene expression or stimulation, all W12 samples showed amplification of *TP53* at the same level as the DNA containing four C-to-T mutations (Fig. 4E), suggesting that the background mutations are present in W12 cells. Results obtained from 3D-PCR of E2, LCR, and *TP53* suggest that A3s may selectively hypermutate viral DNA in W12 cells and that E2 hypermutation may involve a mechanism other than the proposed catabolic hypermutation (39).

IFN-β initiates E2 hypermutation through APOBEC3 expression. Since overexpression of A3A and A3G induced E2 hypermutation in UNG-inhibited W12 cells (Fig. 3) and IFN-β upregulated expression of A3s (Fig. 1B), we next examined whether endogenous A3A and A3G cause E2 hypermutation. The UGI-ER transfectants were cultured in the presence of IFN-β and OHT, and E2 hypermutation was examined by the E2 3D-PCR assays. 3D-PCR of the IFN-β-treated samples showed clear but modest amplification of the E2 gene at a denaturation temperature (84.6°C) lower than that of the negative-control DNA (86.5°C) and the IFN-β-untreated sample (86.5°C), indicating induction of E2 hypermutation by IFN-β in the UNG-inhibited W12 cells (Fig. 5A). DNA sequencing of the E2 fragments revealed C-to-T hypermutation (Fig. 5B, open box). Dinucleotide context analysis of IFN-β-mediated hypermutation showed CpC as a most frequent mutated dinucleotide (Fig. 5C), consistent with dinucleotide preferences of A3G (16, 32). To assess the contribution of A3A and A3G in IFN-β-mediated hypermutation, we transfected siRNAs against A3A and A3G and then stimulated UGI-ER transfectants with IFN-β in the presence of OHT. RT-qPCR revealed that transfection of siRNAs against A3A (siA3A) and A3G suppressed mRNA levels of A3A and A3G at half and 60% of that in the control siRNA (siCont) transfection, respectively (Fig. 5D). Western blotting reconfirmed the reduction of A3G protein levels in siA3G-transfected samples (Fig. 5E). As shown in Fig. 5F, transfection of siCont, followed by stimulation with IFN-β, resulted in amplification of E2 DNA at lower denaturation temperatures (83.2 and 82.6°C) than n.c. (86.5°C), whereas transfection of siA3G resulted in an increase in the denaturation temperature (85.3°C). Transfection of siA3A resulted in amplification of the E2 gene at denaturation temperatures (83.2 and 83.9°C) slightly higher than those of siCont. Sequences of amplified DNAs at denaturation temperature lower than 86.0°C in Fig. 5F were determined. The results showed that E2 hypermutation detected in the siCont samples was biased toward C-to-T mutations (Fig. 5G), similar to the result shown in Fig. 5B. Hypermutation detected in the siA3G-transfected samples was biased toward the G-to-A mutations (Fig. 5G). Dinucleotide context analysis showed that knockdown of A3G decreased CpC and increased TpC dinucleotide contexts in comparison with that of siCont (Fig. 5H). These results collectively suggest that endogenous A3G contributes to E2 hypermutation following IFN-β stimulation in W12 cells. Meanwhile, the contribution of endogenous A3A may be minor judging by the results of dinucleotide context analysis, knockdown experiments, and its expression level (Fig. 1A, 3, and 5).

Expression of APOBEC3 proteins does not affect episomal HPV16 DNA levels in W12 cells. It has been previously reported that IFN-β downregulates the viral episome level in HPV-positive keratinocytes, including W12 cells (35, 45). To evaluate whether A3s are involved in the reduction of viral DNA by IFN-β, the level of viral DNA was measured by Southern blotting. First, W12 cells were transfected with A3A, A3G (and its mutant), and control (GFP) expression vectors, and 3 days after transfection, total DNA was subjected to Southern blotting. Transfection conditions were exactly the same as those used for observation of A3A- and A3G-dependent hypermutation, as shown in Fig. 3. As shown in Fig. 6A, we observed no obvious reduction in HPV episome levels by overexpression of A3A and A3G. Western blotting was performed to determine transgene expression levels (Fig. 6A, bottom panels).

A3s are proposed to degrade HIV-1 viral DNA through the UNG-initiating BER pathway (2, 16, 55). We determined whether UNG inhibition interferes with the IFN-β-mediated downregulation of viral DNA using UGI-ER transfectants. After 3 days of stimulation with IFN-β and OHT, as indicated in Fig. 6B, total DNA was recovered, and HPV16 DNA levels were determined. Stimulation with 1,000 U/ml IFN-β for 3 days slightly reduced HPV16 DNA levels; however, this reduction was not markedly affected by UNG inhibition (Fig. 6B, lane 3 versus lane 4). These

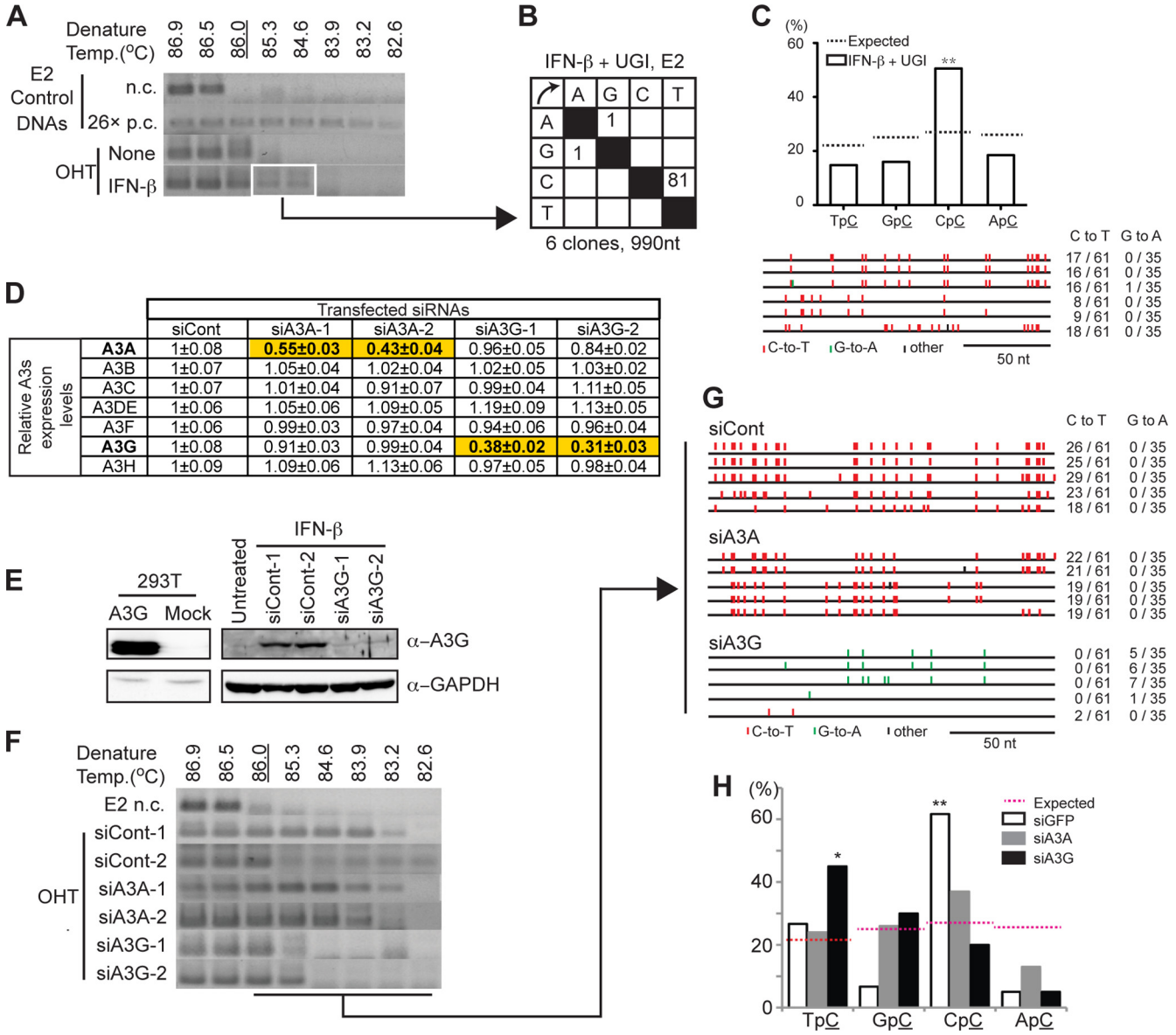

FIG 5 Endogenous APOBEC3 proteins hypermutate E2 in UNG-inhibited W12 cells. (A) UGI-ER transfectants were treated with 1,000 U/ml IFN-β (or were untreated) and 1 μM OHT. After 72 h of incubation, the cells were harvested, and E2 3D-PCR was performed. (B and C) Boxed PCR fragments shown in panel A were excised and cloned into a T vector, and 6 randomly selected clones were sequenced. Detected mutations are shown in panel B, 5′-dinucleotide context analysis is shown in panel C, top, and alignments are shown in panel C, bottom. (D to H) UGI-ER transfectants were transfected with A3A- or A3G-specific (or control) siRNA, and at 6 h after transfection, the cells were treated with 1,000 U/ml IFN-β and 1 μM OHT. After a further 48 h of incubation, cells were harvested and analyzed. (D) Knockdown efficiency for siA3As and siA3Gs and their target specificity. RT-qPCR was performed to measure knockdown efficiency and specificity of siA3A and siA3G transfections. A3 expression levels were normalized to that of HPRT1. The expression level of siCont transfectants was defined as 1. (E) Knockdown efficiency of siA3G was determined by Western blotting. Cell lysate derived from nontagged A3G-transfected 293T cells served as a control. (F) 3D-PCR assay of E2. Total DNA was extracted from siCont-, siA3A-, and siA3G-transfected UGI-ER transfectants was subjected to E2 3D-PCR. (G and H) PCR products amplified at less than 86.0°C, as shown in panel F, were excised and cloned. (G) Results are summarized using alignments. C-to-T and G-to-A hypermutations are indicated as red and green vertical lines, respectively. All other base substitutions are shown as black vertical lines. The number of C-to-T or G-to-A conversions in each sequence is indicated. 5′-dinucleotide context analysis was also performed, as shown in panel H. *, $P < 0.05$; **, $P < 0.01$. n.c., negative-control DNA carrying no mutations. 26× p.c., DNA carrying 26 C-to-T mutations.

data suggest that A3s and UNG do not contribute to a reduction in viral DNA by IFN-β treatment at least under the experimental condition used in this study.

DISCUSSION

A3s are IFN-inducible proteins that restrict reverse transcription-dependent viruses and retrotransposable elements by binding the viral RNP complex, hypermutating nascent DNA, and inhibiting reverse transcription and viral DNA integration (1, 2, 14–16). Vartanian et al. clearly demonstrated that precancerous cervical biopsy samples contain hypermutated HPV DNA (31). However, it has not been shown whether A3 expression is induced in human cervical keratinocytes by IFN stimulation or whether the hypermutated DNA is derived from infected cervical keratinocytes. In

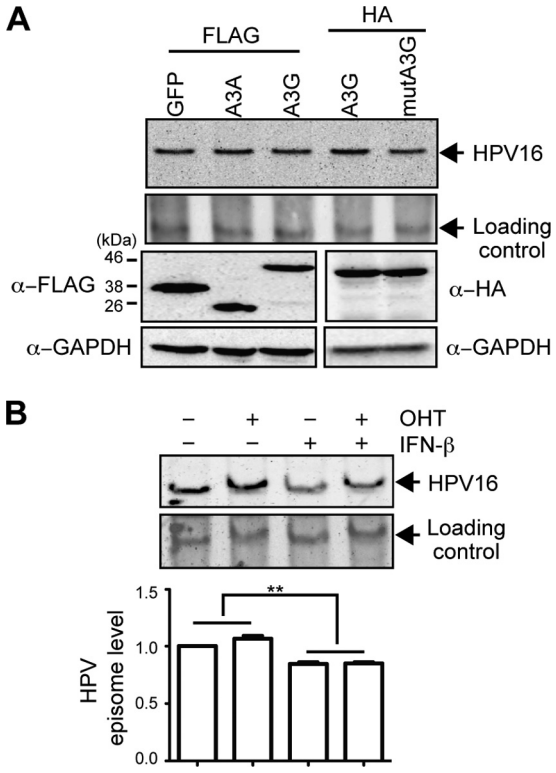

FIG 6 A3G and A3A expression did not change episomal DNA levels in W12 cells. Episomal DNA levels were examined by Southern blotting. (A) W12 cells were transfected with the indicated expression vectors, and 72 h after transfection, total DNA was recovered and digested with BamHI, which cuts once in HPV16 episomal DNA. Fifteen micrograms of the digested total DNA was loaded per lane. The top panel represents linearized HPV16 (7.9 kb), and the second panel shows the loading control by blotting for a particular cellular gene locus. A3A and A3G expression did not change the viral load in the W12 cells. Expression levels of GFP, A3A, and A3G are shown by Western blotting (bottom panels). (B) UGI-ER transfectants were treated with 1 μM OHT and 1,000 U/ml IFN-β, as indicated, and were cultivated for 72 h. Southern blotting was performed as described for panel A. Signal intensities of HPV16 DNA from three independent experiments were normalized to that of the loading control and are indicated at the bottom. The signal in lane 1 (most left line) is defined as 1. **, $P < 0.01$.

the present study using W12 cells, an *in vitro* model for analyzing the early phase of natural HPV16 infection, we investigated whether A3s can hypermutate HPV16 episomal DNA. IFN-β treatment of W12 cells resulted in the upregulation of A3A and A3G mRNA levels and induction of hypermutation in HPV16 DNA (Fig. 1B and 5). Exogenous expression of A3A and A3G induced hypermutation (Fig. 2, 3, and 4), whereas knockdown of endogenous A3A and A3G reduced the hypermutation induced by IFN-β treatment (Fig. 5F). These results suggest that A3G and A3A are responsible for IFN-β-induced E2 hypermutation. However, these hypermutation events are rare because hypermutation can be detected only after enrichment by 3D-PCR (data not shown). Southern blotting of viral DNA did not show reduction of viral replication in A3A- and A3G-expressed W12 cells. In the case of HBV, hypermutation was detected in A3G-expressing hepatocytes even without 3D-PCR, and reduction in HBV viral DNA levels was observed in A3G-overexpressed samples (37). It is possible that hypermutation by A3s may not be sufficiently extensive to cause reduction of viral DNA in W12 cells. A series of *in vitro* studies using purified A3 proteins revealed single-stranded DNA to be an efficient target for A3s (1, 2, 14). We speculate that HPV episomes may not expose a sufficient single-stranded DNA region, and accordingly, poor accessibility of A3s to viral DNA may account for the insufficient accumulation of hypermutations required for antiviral activity of A3s against HPV16. It is also possible that HPV16 has a yet unknown mechanism that inhibits A3 antiviral activity. It is well established that HIV-1 counteracts A3 antiviral activity by a viral protein, Vif (2, 14). Because W12 is an established cell line that stably maintains episomal DNA, it is possible that the virus in this cell line may have overcome the effect of antiviral activities initiated by naive epithelial cells shortly after infection.

Integration of viral DNA into the host genome is an important step in HPV-associated carcinogenesis, and E2 is frequently found disrupted in invasive cervical cancer through viral DNA integration (24, 25). Because the HPV genome does not encode integrase or recombinase that supports viral DNA integration, both viral and cellular DNA need to be cleaved at least once by cellular factors prior to integration. It was previously shown that IFN-β treatment of W12 cells induces clearance of HPV16 episomes from cell populations and facilitates the emergence of cell clones harboring integrated HPV16 DNA (35), suggesting that such DNA cleavages may be induced following IFN-β stimulation. Interestingly, our data demonstrate that IFN-β treatment of W12 cells results in the accumulation of C-to-U conversions in the E2 gene through the deaminase activity of A3s (Fig. 5A and B). Moreover, we showed that UGI enabled an increase in detectable C-to-U conversion generated by A3s (Fig. 3C). Uracil bases in Ig genes generated by AID are converted into DNA double-strand breaks through the UNG-mediated BER pathway, and the resulting DNA ends are resolved as class switch recombination, gene conversion, and chromosomal translocation (3, 4, 6). We analogously speculate that uracil bases in the E2 gene generated by A3s may result in DNA strand breaks, leading to viral DNA integration. Moreover, it was recently reported that A3A and A3B expression induces DNA double-strand breaks and genomic instability (13, 54, 56). DNA strand breaks in viral DNA and host genomic DNA may synergistically increase the chance of viral DNA integration. Although E2 hypermutation is an infrequent event in W12 cells, if this could induce viral DNA integration, it would have a significant impact on facilitating oncogenesis because enhanced expression of E6 and E7 oncogenes from the E2-disrupted integrated HPV genome may transform keratinocytes and give them growth advantage in the cell population (22, 25, 50).

Another potential role of A3s in HPV-related oncogenesis is as a source of mutations. Human cancers, including cervical cancer, have a novel form of mutation (called kataegis), in which C-to-T mutations are clustered in a small genomic region (11, 12). A3A and A3B introduce these kataegis mutations (8–10, 13). In the present study, we demonstrated that A3A expression is induced by IFN-β stimulation and that A3A induces E2 hypermutation in W12 cells (Fig. 1 and 5). Although we did not detect A3A-dependent *TP53* hypermutations, it is possible for A3A to mutate other genomic regions and to play a mutagenic role in HPV-related oncogenesis. Further studies are required to elucidate the role of A3s in HPV-related oncogenesis.

ACKNOWLEDGMENTS

We thank Paul Lambert for providing the W12 cell line. We also thank M. Imayasu and M. Shimadzu for technical support.

This study was supported by the Founding Program for Next Generation World-Leading Researchers, a Grant-in-Aid for Scientific Research on Priority Areas "Cancer," and a Grant-in-Aid for Young Scientists (B) and Research Activity Start-Up from the Japan Society for the Promotion of Science. We declare no conflicts of interest.

REFERENCES

1. **Harris RS, Liddament MT.** 2004. Retroviral restriction by APOBEC proteins. Nat. Rev. Immunol. **4:**868–877. http://dx.doi.org/10.1038/nri1489.
2. **Goila-Gaur R, Strebel K.** 2008. HIV-1 Vif, APOBEC, and intrinsic immunity. Retrovirology. **5:**51. http://dx.doi.org/10.1186/1742-4690-5-51.
3. **Pavri R, Nussenzweig MC.** 2011. AID targeting in antibody diversity. Adv. Immunol. **110:**1–26. http://dx.doi.org/10.1016/B978-0-12-387663-8.00005-3.
4. **Petersen-Mahrt S.** 2005. DNA deamination in immunity. Immunol. Rev. **203:**80–97. http://dx.doi.org/10.1111/j.0105-2896.2005.00232.x.
5. **Muramatsu M, Kinoshita K, Fagarasan S, Yamada S, Shinkai Y, Honjo T.** 2000. Class switch recombination and hypermutation require activation-induced cytidine deaminase (AID), a potential RNA editing enzyme. Cell **102:**553–563. http://dx.doi.org/10.1016/S0092-8674(00)00078-7.
6. **Ganesh K, Neuberger MS.** 2011. The relationship between hypothesis and experiment in unveiling the mechanisms of antibody gene diversification. FASEB J. **25:**1123–1132. http://dx.doi.org/10.1096/fj.11-0402ufm.
7. **Okazaki IM, Hiai H, Kakazu N, Yamada S, Muramatsu M, Kinoshita K, Honjo T.** 2003. Constitutive expression of AID leads to tumorigenesis. J. Exp. Med. **197:**1173–1181. http://dx.doi.org/10.1084/jem.20030275.
8. **Burns MB, Temiz NA, Harris RS.** 2013. Evidence for APOBEC3B mutagenesis in multiple human cancers. Nat. Genet. **45:**977–983. http://dx.doi.org/10.1038/ng.2701.
9. **Roberts SA, Lawrence MS, Klimczak LJ, Grimm SA, Fargo D, Stojanov P, Kiezun A, Kryukov GV, Carter SL, Saksena G, Harris S, Shah RR, Resnick MA, Getz G, Gordenin DA.** 2013. An APOBEC cytidine deaminase mutagenesis pattern is widespread in human cancers. Nat. Genet. **45:**970–976. http://dx.doi.org/10.1038/ng.2702.
10. **Taylor BJ, Nik-Zainal S, Wu YL, Stebbings LA, Raine K, Campbell PJ, Rada C, Stratton MR, Neuberger MS.** 2013. DNA deaminases induce break-associated mutation showers with implication of APOBEC3B and 3A in breast cancer kataegis. eLife **2:**e00534. http://dx.doi.org/10.7554/eLife.00534.
11. **Nik-Zainal S, Alexandrov LB, Wedge DC, Van Loo P, Greenman CD, Raine K, Jones D, Hinton J, Marshall J, Stebbings LA, Menzies A, Martin S, Leung K, Chen L, Leroy C, Ramakrishna M, Rance R, Lau KW, Mudie LJ, Varela I, McBride DJ, Bignell GR, Cooke SL, Shlien A, Gamble J, Whitmore I, Maddison M, Tarpey PS, Davies HR, Papaemmanuil E, Stephens PJ, McLaren S, Butler AP, Teague JW, Jonsson G, Garber JE, Silver D, Miron P, Fatima A, Boyault S, Langerod A, Tutt A, Martens JWM, Aparicio SAJR, Borg A, Salomon AV, Thomas G, Borresen-Dale AL, Richardson AL, Neuberger MS, Futreal PA, Campbell PJ, Stratton MR, Consortium ICG.** 2012. Mutational processes molding the genomes of 21 breast cancers. Cell **149:**979–993. http://dx.doi.org/10.1016/j.cell.2012.04.024.
12. **Alexandrov LB, Nik-Zainal S, Wedge DC, Aparicio SA, Behjati S, Biankin AV, Bignell GR, Bolli N, Borg A, Borresen-Dale AL, Boyault S, Burkhardt B, Butler AP, Caldas C, Davies HR, Desmedt C, Eils R, Eyfjord JE, Foekens JA, Greaves M, Hosoda F, Hutter B, Ilicic T, Imbeaud S, Imielinsk M, Jager N, Jones DT, Jones D, Knappskog S, Kool M, Lakhani SR, Lopez-Otin C, Martin S, Munshi NC, Nakamura H, Northcott PA, Pajic M, Papaemmanuil E, Paradiso A, Pearson JV, Puente XS, Raine K, Ramakrishna M, Richardson AL, Richter J, Rosenstiel P, Schlesner M, Schumacher TN, Span PN, Teague JW, Totoki Y, Tutt AN, Valdes-Mas R, van Buuren MM, van't Veer L, Vincent-Salomon A, Waddell N, Yates LR, Zucman-Rossi J, Futreal PA, McDermott U, Lichter P, Meyerson M, Grimmond SM, Siebert R, Campo E, Shibata T, Pfister SM, Campbell PJ, Stratton MR.** 2013. Signatures of mutational processes in human cancer. Nature **500:**415–421. http://dx.doi.org/10.1038/nature12477.
13. **Burns MB, Lackey L, Carpenter MA, Rathore A, Land AM, Leonard B, Refsland EW, Kotandeniya D, Tretyakova N, Nikas JB, Yee D, Temiz NA, Donohue DE, McDougle RM, Brown WL, Law EK, Harris RS.** 2013. APOBEC3B is an enzymatic source of mutation in breast cancer. Nature **494:**366–370. http://dx.doi.org/10.1038/nature11881.
14. **Malim MH.** 2009. APOBEC proteins and intrinsic resistance to HIV-1 infection. Philos. Trans. R. Soc. Lond. B Biol. Sci. **364:**675–687. http://dx.doi.org/10.1098/rstb.2008.0185.
15. **Okeoma CM, Lovsin N, Peterlin BM, Ross SR.** 2007. APOBEC3 inhibits mouse mammary tumour virus replication in vivo. Nature **445:**927–930. http://dx.doi.org/10.1038/nature05540.
16. **Chiu YL, Greene WC.** 2008. The APOBEC3 cytidine deaminases: an innate defensive network opposing exogenous retroviruses and endogenous retroelements. Annu. Rev. Immunol. **26:**317–353. http://dx.doi.org/10.1146/annurev.immunol.26.021607.090350.
17. **Nguyen DH, Hu J.** 2008. Reverse transcriptase- and RNA packaging signal-dependent incorporation of APOBEC3G into hepatitis B virus nucleocapsids. J. Virol. **82:**6852–6861. http://dx.doi.org/10.1128/JVI.00465-08.
18. **Harris RS, Sheehy AM, Craig HM, Malim MH, Neuberger MS.** 2003. DNA deamination: not just a trigger for antibody diversification but also a mechanism for defense against retroviruses. Nat. Immunol. **4:**641–643. http://dx.doi.org/10.1038/ni0703-641.
19. **Mangeat B, Turelli P, Caron G, Friedli M, Perrin L, Trono D.** 2003. Broad antiretroviral defence by human APOBEC3G through lethal editing of nascent reverse transcripts. Nature **424:**99–103. http://dx.doi.org/10.1038/nature01709.
20. **Yang B, Chen K, Zhang C, Huang S, Zhang H.** 2007. Virion-associated uracil DNA glycosylase-2 and apurinic/apyrimidinic endonuclease are involved in the degradation of APOBEC3G-edited nascent HIV-1 DNA. J. Biol. Chem. **282:**11667–11675. http://dx.doi.org/10.1074/jbc.M606864200.
21. **zur Hausen H.** 2002. Papillomaviruses and cancer: from basic studies to clinical application. Nat. Rev. Cancer **2:**342–350. http://dx.doi.org/10.1038/nrc798.
22. **Bodily J, Laimins LA.** 2011. Persistence of human papillomavirus infection: keys to malignant progression. Trends Microbiol. **19:**33–39. http://dx.doi.org/10.1016/j.tim.2010.10.002.
23. **Stanley MA, Pett MR, Coleman N.** 2007. HPV: from infection to cancer. Biochem. Soc. Trans. **35:**1456–1460. http://dx.doi.org/10.1042/BST0351456.
24. **Pett M, Coleman N.** 2007. Integration of high-risk human papillomavirus: a key event in cervical carcinogenesis? J. Pathol. **212:**356–367. http://dx.doi.org/10.1002/path.2192.
25. **Hamid NA, Brown C, Gaston K.** 2009. The regulation of cell proliferation by the papillomavirus early proteins. Cell. Mol. Life Sci. **66:**1700–1717. http://dx.doi.org/10.1007/s00018-009-8631-7.
26. **Bulliard Y, Narvaiza I, Bertero A, Peddi S, Rohrig UF, Ortiz M, Zoete V, Castro-Diaz N, Turelli P, Telenti A, Michielin O, Weitzman MD, Trono D.** 2011. Structure-function analyses point to a polynucleotide-accommodating groove essential for APOBEC3A restriction activities. J. Virol. **85:**1765–1776. http://dx.doi.org/10.1128/JVI.01651-10.
27. **Tsuge M, Noguchi C, Akiyama R, Matsushita M, Kunihiro K, Tanaka S, Abe H, Mitsui F, Kitamura S, Hatakeyama T, Kimura T, Miki D, Hiraga N, Imamura M, Takahashi S, Hayses CN, Chayama K.** 2010. G to A hypermutation of TT virus. Virus Res. **149:**211–216. http://dx.doi.org/10.1016/j.virusres.2010.01.019.
28. **Gee P, Ando Y, Kitayama H, Yamamoto SP, Kanemura Y, Ebina H, Kawaguchi Y, Koyanagi Y.** 2011. APOBEC1-mediated editing and attenuation of herpes simplex virus 1 DNA indicate that neurons have an antiviral role during herpes simplex encephalitis. J. Virol. **85:**9726–9736. http://dx.doi.org/10.1128/JVI.05288-11.
29. **Suspene R, Aynaud MM, Koch S, Pasdeloup D, Labetoulle M, Gaertner B, Vartanian JP, Meyerhans A, Wain-Hobson S.** 2011. Genetic editing of herpes simplex virus 1 and Epstein-Barr herpesvirus genomes by human APOBEC3 cytidine deaminases in culture and in vivo. J. Virol. **85:**7594–7602. http://dx.doi.org/10.1128/JVI.00290-11.
30. **Chen H, Lilley CE, Yu Q, Lee DV, Chou J, Narvaiza I, Landau NR, Weitzman MD.** 2006. APOBEC3A is a potent inhibitor of adeno-associated virus and retrotransposons. Curr. Biol. **16:**480–485. http://dx.doi.org/10.1016/j.cub.2006.01.031.
31. **Vartanian JP, Guetard D, Henry M, Wain-Hobson S.** 2008. Evidence for editing of human papillomavirus DNA by APOBEC3 in benign and precancerous lesions. Science **320:**230–233. http://dx.doi.org/10.1126/science.1153201.
32. **Stenglein MD, Burns MB, Li M, Lengyel J, Harris RS.** 2010. APOBEC3

proteins mediate the clearance of foreign DNA from human cells. Nat. Struct. Mol. Biol. **17:**222–229. http://dx.doi.org/10.1038/nsmb.1744.
33. **Stanley MA, Browne HM, Appleby M, Minson AC.** 1989. Properties of a non-tumorigenic human cervical keratinocyte cell line. Int. J. Cancer **43:**672–676. http://dx.doi.org/10.1002/ijc.2910430422.
34. **Kalantari M, Lee D, Calleja-Macias IE, Lambert PF, Bernard HU.** 2008. Effects of cellular differentiation, chromosomal integration and 5-aza-2′-deoxycytidine treatment on human papillomavirus-16 DNA methylation in cultured cell lines. Virology **374:**292–303. http://dx.doi.org/10.1016/j.virol.2007.12.016.
35. **Herdman MT, Pett MR, Roberts I, Alazawi WO, Teschendorff AE, Zhang XY, Stanley MA, Coleman N.** 2006. Interferon-beta treatment of cervical keratinocytes naturally infected with human papillomavirus 16 episomes promotes rapid reduction in episome numbers and emergence of latent integrants. Carcinogenesis **27:**2341–2353. http://dx.doi.org/10.1093/carcin/bgl172.
36. **Nagaoka H, Ito S, Muramatsu M, Nakata M, Honjo T.** 2005. DNA cleavage in immunoglobulin somatic hypermutation depends on de novo protein synthesis but not on uracil DNA glycosylase. Proc. Natl. Acad. Sci. U. S. A. **102:**2022–2027. http://dx.doi.org/10.1073/pnas.0409491102.
37. **Kitamura K, Wang Z, Chowdhury S, Simadu M, Koura M, Muramatsu M.** 2013. Uracil DNA glycosylase counteracts APOBEC3G-induced hypermutation of hepatitis B viral genomes: excision repair of covalently closed circular DNA. PLoS Pathog. **9:**e1003361. http://dx.doi.org/10.1371/journal.ppat.1003361.
38. **Ta VT, Nagaoka H, Catalan N, Durandy A, Fischer A, Imai K, Nonoyama S, Tashiro J, Ikegawa M, Ito S, Kinoshita K, Muramatsu M, Honjo T.** 2003. AID mutant analyses indicate requirement for class-switch-specific cofactors. Nat. Immunol. **4:**843–848. http://dx.doi.org/10.1038/ni964.
39. **Suspene R, Aynaud MM, Guetard D, Henry M, Eckhoff G, Marchio A, Pineau P, Dejean A, Vartanian JP, Wain-Hobson S.** 2011. Somatic hypermutation of human mitochondrial and nuclear DNA by APOBEC3 cytidine deaminases, a pathway for DNA catabolism. Proc. Natl. Acad. Sci. U. S. A. **108:**4858–4863. http://dx.doi.org/10.1073/pnas.1009687108.
40. **Liang G, Kitamura K, Wang Z, Liu G, Chowdhury S, Fu W, Koura M, Wakae K, Honjo T, Muramatsu M.** 2013. RNA editing of hepatitis B virus transcripts by activation-induced cytidine deaminase. Proc. Natl. Acad. Sci. U. S. A. **110:**2246–2251. http://dx.doi.org/10.1073/pnas.1221921110.
41. **Suspene R, Guetard D, Henry M, Sommer P, Wain-Hobson S, Vartanian JP.** 2005. Extensive editing of both hepatitis B virus DNA strands by APOBEC3 cytidine deaminases in vitro and in vivo. Proc. Natl. Acad. Sci. U. S. A. **102:**8321–8326. http://dx.doi.org/10.1073/pnas.0408223102.
42. **Bonvin M, Achermann F, Greeve I, Stroka D, Keogh A, Inderbitzin D, Candinas D, Sommer P, Wain-Hobson S, Vartanian JP, Greeve J.** 2006. Interferon-inducible expression of APOBEC3 editing enzymes in human hepatocytes and inhibition of hepatitis B virus replication. Hepatology **43:**1364–1374. http://dx.doi.org/10.1002/hep.21187.
43. **Pichlmair A, Lassnig C, Eberle CA, Gorna MW, Baumann CL, Burkard TR, Burckstummer T, Stefanovic A, Krieger S, Bennett KL, Rulicke T, Weber F, Colinge J, Muller M, Superti-Furga G.** 2011. IFIT1 is an antiviral protein that recognizes 5′-triphosphate RNA. Nat. Immunol. **12:**624–630. http://dx.doi.org/10.1038/ni.2048.
44. **Begum NA, Kinoshita K, Kakazu N, Muramatsu M, Nagaoka H, Shinkura R, Biniszkiewicz D, Boyer LA, Jaenisch R, Honjo T.** 2004. Uracil DNA glycosylase activity is dispensable for immunoglobulin class switch. Science **305:**1160–1163. http://dx.doi.org/10.1126/science.1098444.
45. **Chang YE, Pena L, Sen GC, Park JK, Laimins LA.** 2002. Long-term effect of interferon on keratinocytes that maintain human papillomavirus type 31. J. Virol. **76:**8864–8874. http://dx.doi.org/10.1128/JVI.76.17.8864-8874.2002.
46. **Terenzi F, Saikia P, Sen GC.** 2008. Interferon-inducible protein, P56, inhibits HPV DNA replication by binding to the viral protein E1. EMBO J. **27:**3311–3321. http://dx.doi.org/10.1038/emboj.2008.241.
47. **Terenzi F, Hui DJ, Merrick WC, Sen GC.** 2006. Distinct induction patterns and functions of two closely related interferon-inducible human genes, ISG54 and ISG56. J. Biol. Chem. **281:**34064–34071. http://dx.doi.org/10.1074/jbc.M605771200.
48. **Noguchi C, Hiraga N, Mori N, Tsuge M, Imamura M, Takahashi S, Fujimoto Y, Ochi H, Abe H, Maekawa T, Yatsuji H, Shirakawa K, Takaori-Kondo A, Chayama K.** 2007. Dual effect of APOBEC3G on hepatitis B virus. J. Gen. Virol. **88:**432–440. http://dx.doi.org/10.1099/vir.0.82319-0.
49. **Prochnow C, Bransteitter R, Chen XS.** 2009. APOBEC deaminases-mutases with defensive roles for immunity. Sci. China C Life Sci. **52:**893–902. http://dx.doi.org/10.1007/s11427-009-0133-1.
50. **Woodman CB, Collins SI, Young LS.** 2007. The natural history of cervical HPV infection: unresolved issues. Nat. Rev. Cancer **7:**11–22. http://dx.doi.org/10.1038/nrc2050.
51. **Doi T, Kinoshita K, Ikegawa M, Muramatsu M, Honjo T.** 2003. De novo protein synthesis is required for the activation-induced cytidine deaminase function in class-switch recombination. Proc. Natl. Acad. Sci. U. S. A. **100:**2634–2638. http://dx.doi.org/10.1073/pnas.0437710100.
52. **Kavli B, Otterlei M, Slupphaug G, Krokan HE.** 2007. Uracil in DNA-general mutagen, but normal intermediate in acquired immunity. DNA Repair **6:**505–516. http://dx.doi.org/10.1016/j.dnarep.2006.10.014.
53. **Shindo K, Takaori-Kondo A, Kobayashi M, Abudu A, Fukunaga K, Uchiyama T.** 2003. The enzymatic activity of CEM15/Apobec-3G is essential for the regulation of the infectivity of HIV-1 virion but not a sole determinant of its antiviral activity. J. Biol. Chem. **278:**44412–44416. http://dx.doi.org/10.1074/jbc.C300376200.
54. **Mussil B, Suspene R, Aynaud MM, Gauvrit A, Vartanian JP, Wain-Hobson S.** 2013. Human APOBEC3A isoforms translocate to the nucleus and induce DNA double strand breaks leading to cell stress and death. PLoS One **8:**e73641. http://dx.doi.org/10.1371/journal.pone.0073641.
55. **Harris RS, Bishop KN, Sheehy AM, Craig HM, Petersen-Mahrt SK, Watt IN, Neuberger MS, Malim MH.** 2003. DNA deamination mediates innate immunity to retroviral infection. Cell **113:**803–809. http://dx.doi.org/10.1016/S0092-8674(03)00423-9.
56. **Lackey L, Law EK, Brown WL, Harris RS.** 2013. Subcellular localization of the APOBEC3 proteins during mitosis and implications for genomic DNA deamination. Cell Cycle **12:**762–772. http://dx.doi.org/10.4161/cc.23713.